

**Externally induced metastability of an electron in a Penning trap: Analytical results**

S. Brouard and J. Plata

*Departamento de Física Fundamental II, Universidad de La Laguna, La Laguna E38204, Tenerife, Spain*

(Received 12 December 2000; published 14 November 2001)

The effect of a driving field on the cyclotron mode of a relativistic electron in a Penning trap is studied analytically. The Hamiltonian dynamics of this driven nonlinear oscillator is analyzed by using linearization techniques and displaced squeezed-state formalism. With the approximate analytical expressions obtained for the eigenstates in this approach, a simplified treatment of the dissipative dynamics is carried out and some of the nontrivial features found in a recent numerical study [D. Enzer and G. Gabrielse, *Phys. Rev. Lett.* **78**, 1211 (1997)] are unraveled. The emergence of different time scales and the generation of a metastable statistical mixture are understood in terms of the changes induced in the structure of the master equation by the nonuniform characteristics of the eigenstates; the partial revivals of specific coherent states are accounted for by the evolution of particular coherences. The control of these effects by a proper choice of the driving parameters is discussed.

DOI: 10.1103/PhysRevA.64.063405

PACS number(s): 32.80.Pj, 42.50.Lc

**I. INTRODUCTION**

The study of trapped electrons, intense in the last decades, has opened up new opportunities for high-precision experiments with important, conceptual and practical implications [1–8]. The advances brought about in the observation techniques and the increasing knowledge of the rich dynamics of these systems have allowed testing fundamental effects ranging from classical noise-induced transitions [4] to quantum jumps [7]. In this line, it is worth mentioning some recent developments that have enlarged the field of applications: it has been shown that an electron in a Penning trap provides a realizable scenario for implementing quantum nondemolition measurement [7]; additionally, the potential applicability of this system in generation of macroscopic quantum-interference states [5] and in quantum computing [6] has been discussed. Presently, considerable attention is being paid to the effects of dissipation, an important aspect of the dynamics, which, apart from having intrinsic fundamental interest, is crucial for the practicality of some of the proposed applications.

This work focuses on the dissipative dynamics of an electron interacting with a circularly-polarized oscillating electric field in a Penning trap; our objective is the analytical explanation of the nontrivial behavior revealed by a recent numerical study [1]. It has been shown [1] that, as a result of the combined action of the external field and the nonlinear potential that accounts for relativistic corrections, the cyclotron mode, described as a driven quartic oscillator coupled to a reservoir, presents complex damping processes. Strongly nonuniform characteristics of the dynamics, partially reflected in the bistability of the classical configuration space, have been uncovered: various time scales are present in sequences that change as the initial preparation is varied with metastability occurring for initial conditions linked to the basin of one of the “attractors.” Significantly, the evolution of a coherent state centered on that fixed point displays the following features: partial revivals in the initial stage, the subsequent emergence of a highly populated metastable state, and the eventual decay to the central area of the phase

space. It is remarkable that, for the range of parameters considered, the quantum system, as opposed to its bistable classical analog, is asymptotically monostable.

In previous studies [1,3] different theoretical approaches have been developed to account for these findings and, in fact, important points have been clarified. However, there are still some questions that deserve additional analytical work; specifically, an explanation for the revivals and a better characterization of the asymptotic evolution are needed. Here, we aim at giving a more complete understanding of these effects. In our approach, the analysis of the classical counterpart gives the clues to setting up unitary transformations that allow an effective reduction of the Hamiltonian dynamics near the fixed points and provide a suitable framework for tackling the open system: with a simplified treatment of the master equation, some of the mechanisms underlying the dynamics are identified and part of the numerical results are reproduced analytically.

The outline of the paper is as follows. The Hamiltonian system is analyzed in Sec. II: approximate expressions are given for some of the energy eigenstates. Section III deals with dissipation: it is shown how the unitary transformations introduced in the previous section alter the functional structure of the master equation, explaining the different time scales present in the decay processes and the generation of metastable states. Some strategies of control are discussed in Sec. IV. Finally, in Sec. V our conclusions are summarized.

**II. THE HAMILTONIAN DYNAMICS**

We consider a harmonic oscillator of frequency  $\omega_c$  perturbed by a quartic nonlinear term and driven by a circularly polarized classical field. In the rotating frame of the driving field the system is defined by [1,3]

$$H = \hbar(\omega_c - \omega) \left( a^\dagger a + \frac{1}{2} \right) - \frac{1}{2} \hbar \delta \left( a^\dagger a + \frac{1}{2} \right)^2 + \frac{1}{2} \hbar \Omega_R (e^{i\varphi} a + e^{-i\varphi} a^\dagger), \quad (1)$$

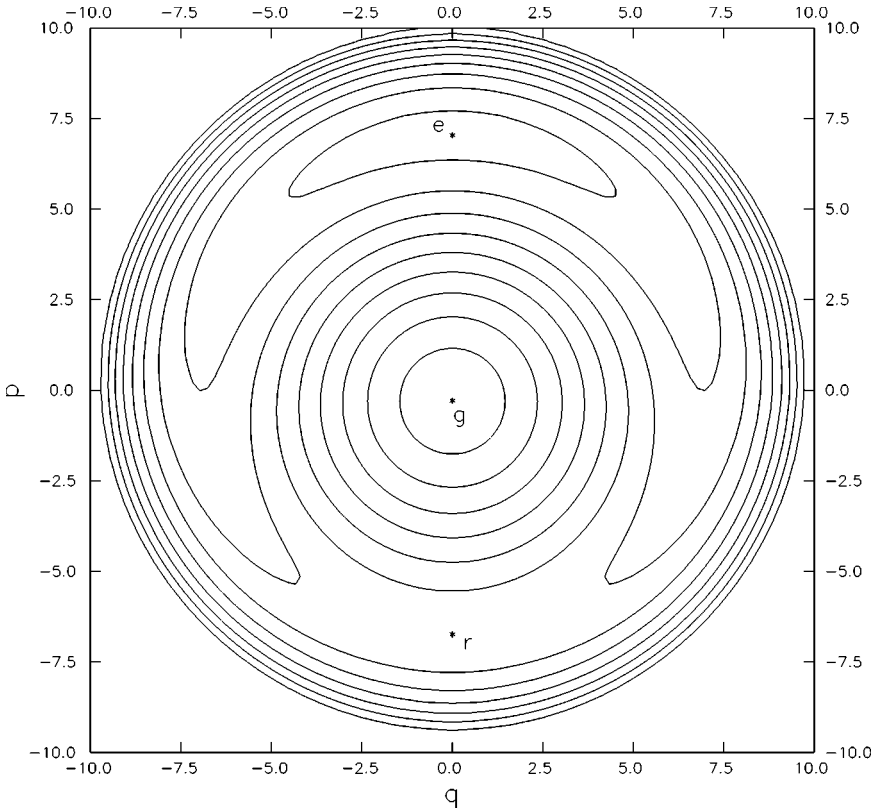


FIG. 1. Phase space for the system defined by Eq. (2) with the parameters  $\Delta = 48\delta$ ,  $\Omega_R = 28\delta$ , and an arbitrary scale factor. The same parameters are used in all the figures.

where  $\delta$  is the anharmonicity parameter and  $\omega$ ,  $\Omega_R$ , and  $\varphi$  denote, respectively, drive frequency, Rabi frequency, and initial phase of the external field. Without loss of generality, we take, as in Ref. [1],  $\varphi = -\pi/2$ ; in our study, it will be clear that a different value for  $\varphi$  would simply mean a change in the angular position of the metastable state. This Hamiltonian describes the cyclotron mode of an electron in a Penning trap, the elimination of the axial and magnetron modes being allowed by the magnitude of their respective time scales [1]; the nonlinear term accounts for the relativistic corrections and the driving term characterizes the interaction with an electric field. Note that  $H$  corresponds also to a driven electromagnetic mode in a cavity with an intensity-dependent refractive index; indeed, in a certain range of parameters, it represents a typical scenario for dispersive optical bistability [9–12].

Let us see how the analysis of the phase space provides us with information relevant to obtaining some of the energy eigenstates. The Hamiltonian function of the classical counterpart can be defined from the diagonal-matrix elements of  $H$  in the coherent state representation  $\{|\alpha\rangle\}$ ; taking  $q = \text{Re}(\alpha)$  and  $p = \text{Im}(\alpha)$ , it reads

$$H_{cl} \equiv \langle \alpha | H | \alpha \rangle = \Delta(p^2 + q^2) - \frac{1}{2} \delta(p^2 + q^2)^2 + \Omega_R p, \quad (2)$$

with  $\Delta = \omega_c - \omega - \delta/2$  and where, as in the rest of the paper, we have dropped the zero-point energy and have taken  $\hbar = 1$ . In the regime where the nontrivial quantum features have been detected this classical system (see the phase space depicted in Fig. 1) has three fixed points [3]:  $g$  is a local minimum,  $e$  is a local maximum, and  $r$  is a saddle point.

Near  $g$  the system can be approximated as a harmonic oscillator; additionally, despite the fact that  $e$  is a maximum and because of the specific characteristics of the nonlocal potential, a harmonic approximation for the Hamiltonian function around  $e$  is also possible. Note that the bistable character is linked to the different signs of the harmonic and anharmonic contributions.

From these results, we set up the following strategy to solve the quantum system. First, we perform a unitary transformation with the displacement operator  $D(v) \equiv \exp(va^\dagger - v^*a)$  [13,14] and calculate, through a reduction procedure that parallels the classical treatment, the three values of  $v$  that define the quantum analogs of the fixed points. Second, the validity of a harmonic approximation for each of the three differently displaced Hamiltonians is studied and analytical expressions are obtained for the eigenstates when the linearization is valid. Finally, the effect of the nonlinear terms is analyzed.

Accordingly, we first apply  $D(v)$ ; the resulting Hamiltonian  $H(v) \equiv D^\dagger(v)HD(v)$  takes the form

$$\begin{aligned} H(v) = & (\Delta - 2\delta|v|^2)a^\dagger a + \left\{ \left[ \left( \Delta - \frac{\delta}{2} \right) v - \delta|v|^2 v + \frac{\Omega_R}{2} \right] a^\dagger \right. \\ & \left. - \frac{1}{2} \delta v^2 a^{\dagger 2} + \text{H.c.} \right\} - \frac{1}{2} \delta (a^\dagger a)^2 \\ & + [-\delta v a^\dagger a^\dagger a + \text{H.c.}], \end{aligned} \quad (3)$$

where H.c. stands for Hermitian conjugate. Now, proceeding to obtain the displacements  $v$  from which a linearization of

the system may be valid, we make the coefficients of  $a$  and  $a^\dagger$  in the above equation equal to zero, that is, we impose

$$\left(\Delta - \frac{\delta}{2}\right)v - \delta|v|^2v + \frac{\Omega_R}{2} = 0. \quad (4)$$

It is worth making some comments here. First, note that this equation implies the absorption of the driving term into the new representation, which is a necessary first step in our approach given the nonperturbative character of the driving field. For  $\delta=0$ , that is, for a driven linear oscillator, Eq. (4) becomes a first-order equation in  $v$ ; it can be solved to obtain the displacement parameter of the displaced states  $D(v)|n\rangle$  that exactly diagonalizes the system in the original representation; the number states  $|n\rangle$  are, in this particular case, eigenstates of  $H(v)$ . Second, for our nonlinear system, this condition parallels the requirement of zero net force that determines the classical fixed points. In fact, this is a necessary condition for the classical linearization; it is not sufficient, though, since the expansion of a classical Hamiltonian about a fixed point can be approximated as a harmonic oscillator only when the second-order terms in the expansion correspond to a harmonic potential. In this sense, we stress that, in our quantum system, the validity of a harmonic approximation around each of the three fixed points will be determined by analyzing if the quadratic terms  $-1/2\delta v^2 a^{\dagger 2} + \text{H.c.}$ , present in Eq. (3) can be incorporated, through proper unitary transformation [15], into a Hamiltonian with the simplest harmonic-functional form, i.e., if they correspond to standard terms of squeezing [15,16]. If the linearization is feasible, we will evaluate the relative magnitude of the rest of the contributions, namely, the quartic anharmonic part,  $-1/2\delta(a^\dagger a)^2$  and the residual nonlinear terms,  $-\delta v a^\dagger a^\dagger a + \text{H.c.}$ , their inclusion in our scheme in the right perturbative order being subsequently implemented.

To illustrate the applicability of this methodology, let us consider the parameters  $\Delta = 48\delta$  and  $\Omega_R = 28\delta$ , which correspond to one of the cases studied in Ref. [1]. Equation (4) gives then for the displacements:  $v_g = -0.295i$ ,  $v_e = 7.035i$ , and  $v_r = -6.74i$ ; as our notation suggests, they can be related to the classical fixed points. Actually, the analogy goes further and parallel treatments can be carried out for both, classical and quantum, systems. Our strategy proceeds as follows:

(i) In the Hamiltonian  $H(v_g)$ , which results from applying  $D(v_g)$ , the squeezing terms,  $-1/2\delta v_g^2 a^{\dagger 2} + \text{H.c.}$ , can be neglected in first order since  $v_g^2 \ll 1$ . Hence, the local dynamics, including the effects of the quartic nonlinear term  $-1/2\delta(a^\dagger a)^2$ , can be approximated by the anharmonic oscillator defined by

$$H_g^{ef} = (\Delta - 2\delta|v_g|^2)a^\dagger a - \frac{1}{2}\delta(a^\dagger a)^2. \quad (5)$$

In effect,  $D(v_g)|n\rangle$ , eigenstates of this effective Hamiltonian in the original representation, give excellent approximations to some of the eigenstates of the complete system. This result is particularly relevant to the dissipative dynamics, since, as we will show later on,  $D(v_g)|0\rangle$  is the asymptotic state of

the open system at zero temperature. We recall that a displaced vacuum is also the stationary state of the dissipative driven-linear oscillator.

Let us evaluate now the effect of the additional nonlinear terms  $-\delta v a^\dagger a^\dagger a + \text{H.c.}$  Since, apart from constants, they are given by the product of the number operator and either the annihilation or the creation operator, their effect could be partially understood as leading to a number-dependent displacement. Accordingly, we build up optimized eigenstates as displaced states  $D[v_g(n)]|n\rangle$  with the displacement parameter depending on the occupation number. By applying Hamiltonian of Eq. (3) to the Fock states  $|n\rangle$  and ignoring the effect of the squeezing terms, it is straightforwardly shown that these states approximately satisfy the eigenstate condition for the values of  $v_g(n)$  given by

$$\left[\Delta - \delta\left(\frac{1}{2} + n\right)\right]v_g(n) - \delta|v_g(n)|^2v_g(n) + \frac{\Omega_R}{2} = 0, \quad (6)$$

and that, consequently, the states  $D(v_g(n))|n\rangle$  are approximate eigenstates in the original representation. Note that, in the above equation,  $n$  comes from the contribution of the number operator that appears as a factor in the additional nonlinear terms  $-\delta v a^\dagger a^\dagger a + \text{H.c.}$  By taking  $n=0$ , we consistently recover Eq. (4). On the other hand, the solutions for  $n \neq 0$  improve the quality of our previous approximation.

A direct connection between the results of the quantum study and the characteristics of the phase space is provided by the  $Q$  functions [17] (also known as Husimi functions), defined as  $Q(q,p) = \langle \alpha | \rho | \alpha \rangle$ , where  $\rho$  denotes the density operator,  $\alpha$  is the amplitude of the coherent state with  $\text{Re}(\alpha) = q$  and  $\text{Im}(\alpha) = p$ . In Figs. 2, 3, and 4, we plot the analytical Husimi functions [16] for some of the approximate eigenstates  $D(v_g)|n\rangle$  and for the related ‘‘exact’’ eigenstates, obtained through a numerical diagonalization of the matrix representation of the complete Hamiltonian of Eq. (1) in the Fock state basis. The validity of our approach is apparent in these figures. Obviously, the agreement with the numerical results can be improved by working with the optimized eigenstates  $D(v_g(n))|n\rangle$ ; in fact, the optimization procedure is necessary to reproduce eigenstates with  $Q$  functions located in the outer regions of the phase space, beyond the local maximum area. However, in order to give a simple picture of the dissipative processes in the inner region of the phase space, we will work with the approximate eigenstates  $D(v_g)|n\rangle$  in the next section.

(ii) Because of the magnitude of  $v_e$ , the harmonic approximation around the local maximum must necessarily include the standard terms of squeezing,  $-1/2\delta v_e^2 a^{\dagger 2} + \text{H.c.}$  Their explicit treatment is carried out in the usual way: we make a further change of representation through the unitary transformation defined by the squeeze operator  $S(\eta) = \exp[(1/2)(\eta a^2 - \eta^* a^{\dagger 2})]$ , where the squeeze parameter  $\eta$  is obtained by imposing that the linear part of the transformed Hamiltonian  $S^\dagger(\eta)H(v_e)S(\eta)$  has the simplest harmonic-functional form. The squeezing terms are then absorbed into the functional form of the new basis and the resulting transformed linear Hamiltonian reads

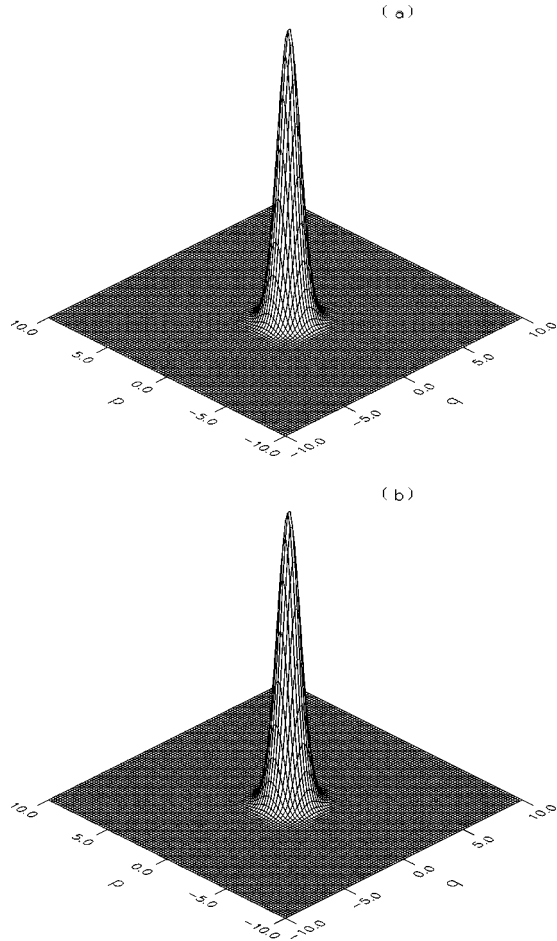


FIG. 2.  $Q$  functions for the approximate eigenstate  $D(v_g)|0\rangle$  ( $v_g = -0.295i$ ) (a) and for the corresponding exact eigenstate (b).

$$H_e^{ef} = [(\Delta - 2\delta|v_e|^2)\cosh 2s + \delta\sinh 2s \operatorname{Re}(v_e^2 e^{-i\theta})] a^\dagger a, \quad (7)$$

where  $s$  and  $\theta$  are related to the squeeze parameter through  $\eta = |\eta|e^{i\theta} \equiv s e^{i\theta}$ . For the example considered in this paper, we get  $\eta = -1.053$ . Of course, neglecting in first order the effect of the nonlinear part,  $-1/2\delta(a^\dagger a)^2 + (-\delta v_e a^\dagger a^\dagger a + \text{H.c.})$ , is justified only for small occupation numbers. It will be shown further on that, despite this approximation, the eigenstates found,  $D(v_e)S(\eta)|n\rangle$ , have the basic characteristics needed to explain part of the features of the dissipative behavior; some of the associated Husimi functions, also obtained analytically [16], can be compared in Figs. 5, 6, and 7 with the ones corresponding to the numerical exact eigenstates.

(iii) Finally, for  $v_r$ , a harmonic approximation is not possible: the quadratic terms in  $H(v_r)$  do not correspond to a harmonic oscillator (see Ref. [15] for details), as it could have been guessed, given the saddle character of the associated fixed point. Hence, a local study of the dynamics in this area of the phase space is not allowed.

Let us summarize the results of this section. Two sets of approximate eigenstates have been found: displaced squeezed number states  $D(v_e)S(\eta)|n\rangle$ , with  $Q$  functions in the region of the local maximum; and displaced states

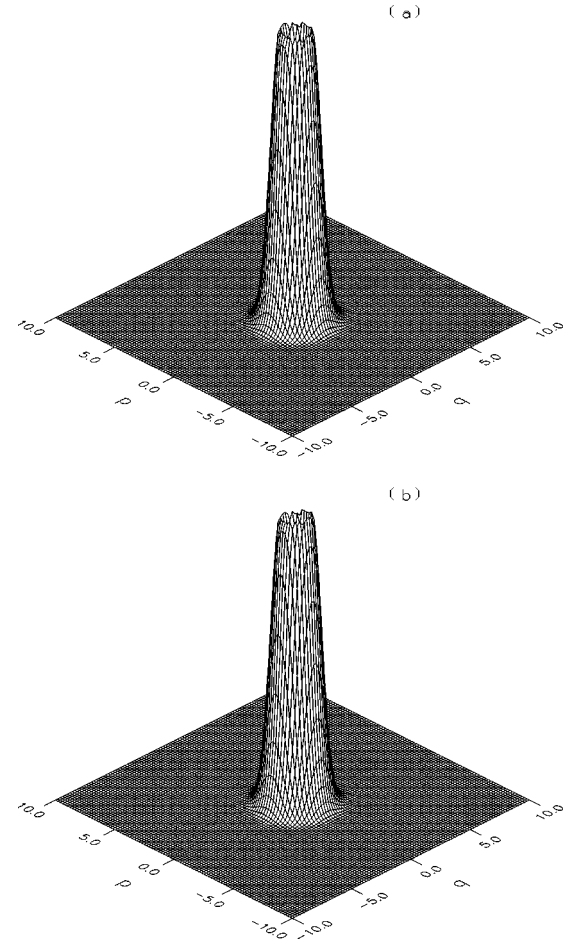


FIG. 3. Same caption as Fig. 2, for the approximate eigenstate  $D(v_g)|1\rangle$ .

$D(v_g(n))|n\rangle$ ,  $v_g(n)$  varying smoothly with  $n$ , which correspond to eigenstates with  $Q$  functions located in the central and outer regions, where the squeezing can be neglected in first order. In both cases, the analytical approach, which reproduces accurately several eigenvalues and gets worse as the occupation number increases, can certainly be improved by including higher-order effects, needed, for example, to guarantee the orthogonality of the complete representation. Nevertheless, in order to simplify the unraveling of the peculiar damping processes, which is the main objective of the next section, we go on working at the presented level of approximation.

From the previous analysis, an explanation for one of the main findings of Ref. [1] can be guessed: a coherent state centered on the local maximum experiences partial revivals because, for the set of parameters chosen, it is basically a superposition of two eigenstates, i.e.,  $|v_e\rangle = D(v_e)|0\rangle = c_1 D(v_e)S(\eta)|0\rangle + c_2 D(v_e)S(\eta)|2\rangle$ , which, therefore, oscillates between the symmetric and the antisymmetric combinations. The energy splitting, which determines the oscillation period (time of revival) through  $t_{rev} = 2\pi/\Delta E$ , can be straightforwardly obtained as  $\Delta E = 2[(\Delta - 2s\delta|v_e|^{2s})\cosh 2s + \delta\sinh 2s \operatorname{Re}(v_e^2 e^{-i\theta})]$  [see Eq. (7)]. Consequently, taking into account that  $\tanh(2s) = -\delta|v_e|^{2s}/(\Delta - 2s\delta|v_e|^{2s})$  and  $\theta = \pi$ , the time of revival can



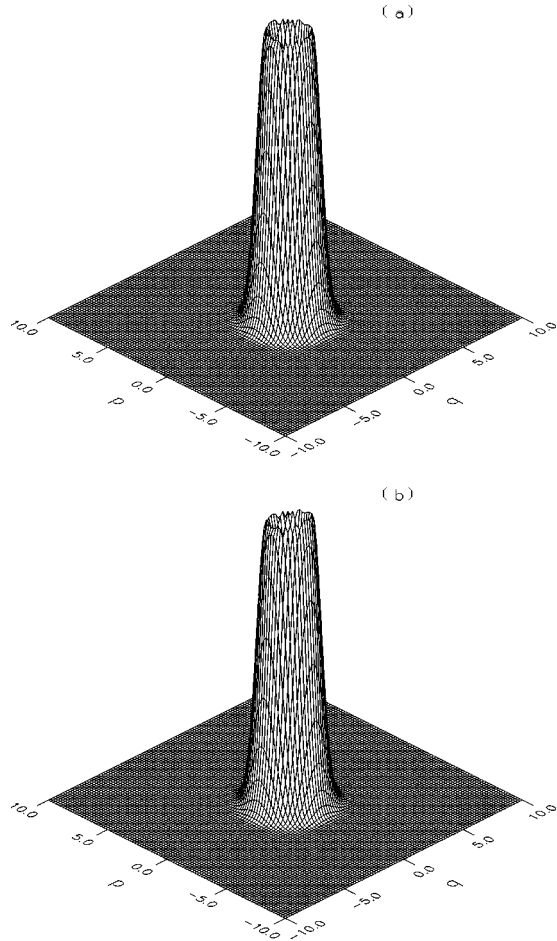


FIG. 4. Same caption as Fig. 2, for the approximate eigenstate  $D(v_e)|2\rangle$ .

be approximated in our analytical framework as  $t_{rev} \sim \pi/\sqrt{\delta\Omega_n}$ , where  $\Omega_n$  is an effective Rabi frequency defined as  $\Omega_n = \Omega_R \bar{n}^{1/2}$  and  $\bar{n} = |v_e|^2$  is the mean-occupation number of the coherent state. This result is one of the main achievements of the present work; its excellent agreement with the time of revival obtained in Ref. [1] from a numerical study, confirms the validity of the treatment presented. Later on, it will be shown that in the open system, the damping of the corresponding coherence leads to the eventual disappearance of the revivals.

Let us close this discussion by pointing out some other, qualitative, aspects of the evolution of  $D(v_e)|0\rangle$ . First, note that the considerable localization of this state, i.e., the fact that the evolution of the corresponding  $Q$  function is restricted to a small area of the phase space, is due to the approximate linear character of the system around the maximum. This point can be clarified if we artificially make  $\eta = 0$  in our previous results:  $D(v_e)|0\rangle$  then becomes an eigenstate of the local harmonic oscillator and, consequently, experiences a complete time localization. Hence, we can also conclude that it is the presence of squeezing that gives the partial character to the actual localization, the revivals being rooted in the strong overlapping of the state with two of the eigenstates. Finally, we point out that our approach allows us to conjecture the almost exact localization of an initially pre-

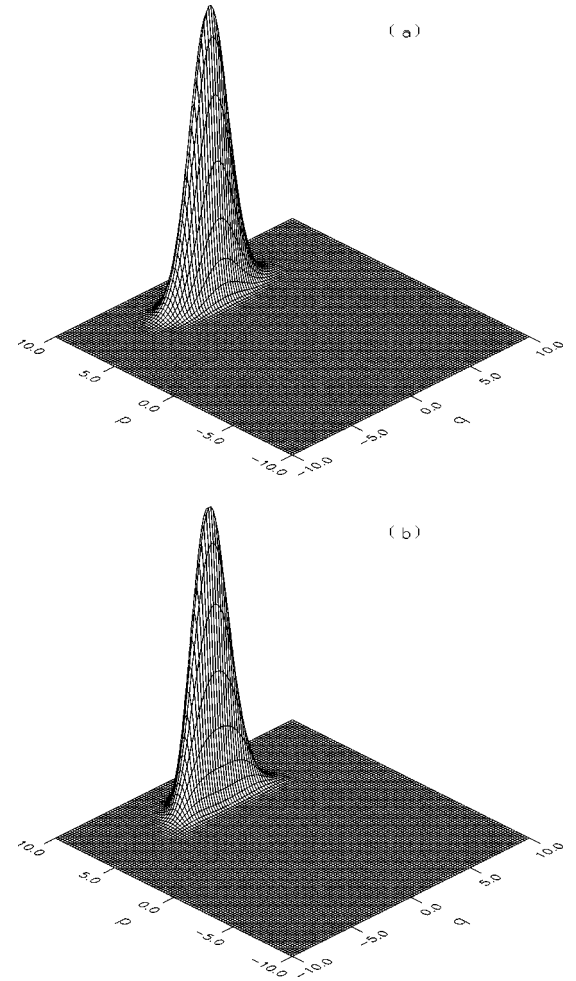


FIG. 5.  $Q$  functions for the approximate eigenstate  $D(v_e)S(\eta)|0\rangle$  ( $v_e = 7.035i$  and  $\eta = -1.053$ ) (a) and for the corresponding exact eigenstate (b).

pared state  $D(v_e)S(\eta)|0\rangle$ . Actually, this feature is not robust against dissipation since the coupling to a reservoir leads, as we will show in the next section, to a different asymptotic state, even at zero temperature.

### III. THE DISSIPATIVE DYNAMICS

Dissipation is included in our model by linearly coupling the system to a thermal reservoir of harmonic oscillators. Once the standard, Born-Markov and rotating-wave approximations [17,18] have been made and the partial trace over the bath variables has been taken, the reduced system is described by the master equation

$$\begin{aligned} \frac{d\rho}{dt} = & -i[H, \rho] + \frac{\gamma_c}{2} (2a\rho a^\dagger - a^\dagger a \rho - \rho a^\dagger a) + \bar{N} \gamma_c (a^\dagger \rho a \\ & + a \rho a^\dagger - a^\dagger a \rho - \rho a a^\dagger), \end{aligned} \quad (8)$$

where  $H$  is given by Eq. (1);  $\gamma_c$  is the damping constant, which depends on the coupling strength and on the spectral density of the reservoir at the oscillator frequency  $\omega_c$ ; and  $\bar{N}$  is the thermal mean-occupation number of the bath. As

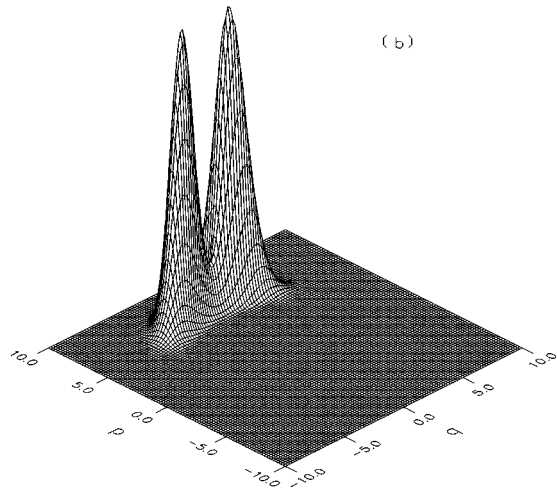
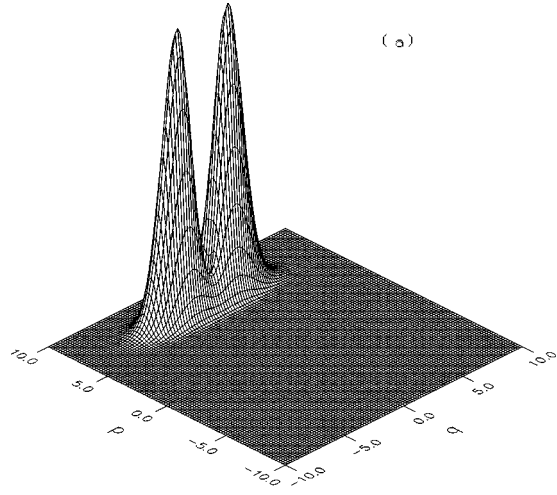


FIG. 6. Same caption as Fig. 5, for the approximate eigenstate  $D(v_e)S(\eta)|1\rangle$ .

shown in Ref. [19], this description is valid only for a small nonlinearity, which is precisely the case considered here, i.e.,  $\delta \ll \omega_c$ .

The above equation was solved numerically in Ref. [1]; also, a semiclassical approach for the evolution of the corresponding  $Q$  function was presented in Ref. [3]. Given the complexity of the problem, evident in those studies and the consequent difficulty in obtaining complete analytical solutions, we have opted here to focus on the characteristics of the system near the attractors and gain insight into some of the unexplained dissipative features by using our knowledge of the deterministic dynamics. A strategy formally convenient for reaching this objective consists of working first with a simplified version of the model and then extrapolating part of the results to the complete system. Specifically, being consistent with the local character of our previous analysis, we study the system whose Hamiltonian dynamics is exactly described either by  $H_g^{ef}$  in the basis  $\{D(v_g)|n\rangle\}$ , or by  $H_e^{ef}$  in the basis  $\{D(v_e)S(\eta)|n\rangle\}$ , the relevance of each description being unambiguously determined by the initial preparation. Additionally, we assume that in both cases a master equation with the functional form given by Eq. (8) accounts for dissipation. In the following, it will be clear that despite its arti-

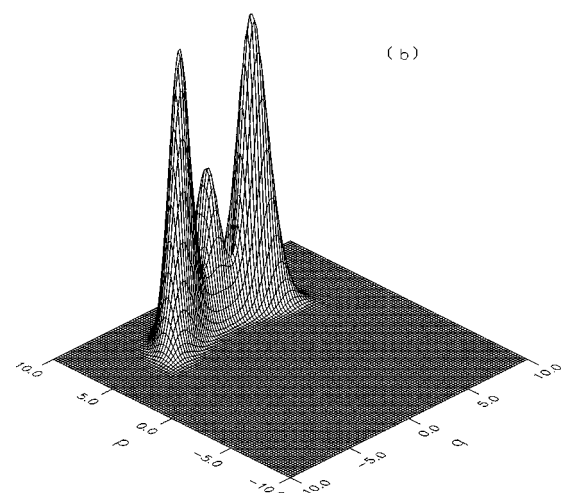
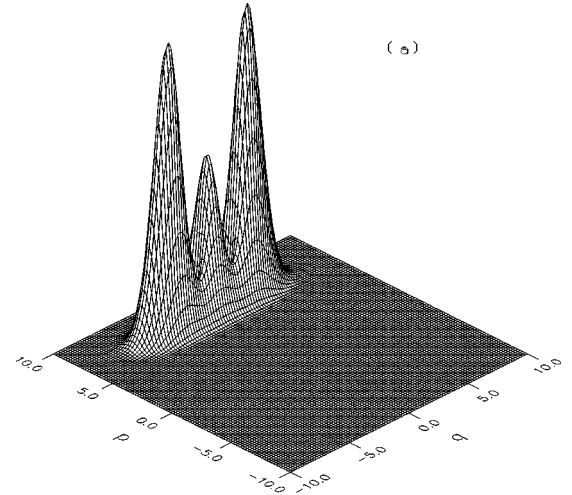


FIG. 7. Same caption as Fig. 5, for the approximate eigenstate  $D(v_e)S(\eta)|2\rangle$ .

ficial character, this model, built up with two representations that give only approximate expressions for part of the “exact” eigenstates and where bistability has been introduced *ad hoc*, is suitable to clarify the asymptotic behavior and some of the properties of the metastable state. Hence, let us make a parallel treatment of the changes induced in the structure of the master equation by the unitary transformations  $D(v_g)$  and  $D(v_e)S(\eta)$ .

#### A. The master equation in the displaced state basis

When Hamiltonian dynamics is described by  $H_g^{ef}$ , the time evolution of  $\tilde{\rho} = D^\dagger(v_g)\rho D(v_g)$  in the corresponding open system is readily obtained as

$$\begin{aligned} \frac{d\tilde{\rho}}{dt} = & -i[H_g^{ef}, \tilde{\rho}] + \frac{\gamma_c}{2}(2a\tilde{\rho}a^\dagger - a^\dagger a\tilde{\rho} - \tilde{\rho}a^\dagger a) \\ & + \bar{N}\gamma_c(a^\dagger\tilde{\rho}a + a\tilde{\rho}a^\dagger - a^\dagger a\tilde{\rho} - \tilde{\rho}a a^\dagger). \end{aligned} \quad (9)$$

In deriving this equation we have neglected the terms whose order of magnitude is given by  $\gamma_c v_g$ , as they merely imply a

second-order correction. There are analytical solutions to this equation [20–22]; a well-known result, with a significant importance for our study, is that the Gaussian  $Q$  function of an initial coherent state evolves into a ring of probability with a decreasing radius, a Gaussian  $Q$ -function being eventually formed at the center of the phase space. For  $T=0$ , this asymptotic state corresponds to the vacuum; in the untransformed representation, it is the displaced vacuum  $D(v_g)|0\rangle$  or, equivalently, the coherent state  $|v_g\rangle$  whose amplitude is given by the displacement parameter. For a nonzero temperature, the final state is a statistical mixture of the states  $D(v_g)|n\rangle$ , populated according to the corresponding Boltzmann factors.

### B. The master equation in the displaced squeezed state basis

Conversely, if Hamiltonian dynamics is described by  $H_e^{ef}$ , the dissipative processes can be properly studied in terms of  $\tilde{\rho} = S^\dagger(\eta)D^\dagger(v_e)\rho D(v_e)S(\eta)$ , whose time evolution reads

$$\begin{aligned} \frac{d\tilde{\rho}}{dt} = & -i[H_e^{ef}, \tilde{\rho}] + \frac{\gamma_c}{2} \cosh^2 s (2a\tilde{\rho}a^\dagger - a^\dagger a\tilde{\rho} - \tilde{\rho}a^\dagger a) \\ & + \frac{\gamma_c}{2} \sinh^2 s (2a^\dagger \tilde{\rho}a - a^\dagger a\tilde{\rho} - \tilde{\rho}a^\dagger a - 2\tilde{\rho}) + \frac{\gamma_c}{4} \sinh 2s \\ & \times (-2e^{-i\theta} a\tilde{\rho}a + e^{-i\theta}(a^2\tilde{\rho} + \tilde{\rho}a^2) + \text{H.c.}). \end{aligned} \quad (10)$$

To present the physical mechanisms in the simplest way, we have taken  $T=0$  and, again, have suppressed the second-order corrections. This expression defines a behavior qualitatively different from the one given by Eq. (9): the unitary transformation  $S(\eta)$ , in addition to changing the effective decay rates, which become dependent on the squeeze parameter, alters the structure of the master equation, leading to a significantly different asymptotic state. In particular regimes, we can go further on this point: the description simplifies considerably if the differences between the eigenenergies of  $H_e^{ef}$  are much larger than the damping constant, which is the case for the parameters chosen to illustrate our methodology, i.e.,  $\Delta = 48\delta$ ,  $\Omega_R = 28\delta$ , and  $\gamma_c \ll \delta$ . Then, as the coherences oscillate in a time scale much smaller than the characteristic time for the evolution of the populations,  $\sim 1/\gamma_c$ , they can be averaged to zero in the population equation. Consequently, we derive

$$\begin{aligned} \dot{\tilde{\rho}}_{n,n} = & \frac{\gamma_c}{2} (\cosh^2 s) [2(n+1)\tilde{\rho}_{n+1,n+1} - 2n\tilde{\rho}_{n,n}] + \frac{\gamma_c}{2} (\sinh^2 s) \\ & \times [2n\tilde{\rho}_{n-1,n-1} - 2(n+1)\tilde{\rho}_{n,n}]. \end{aligned} \quad (11)$$

Moreover, as the coherences eventually decay to zero, the asymptotic state, in the considered case of zero temperature, is easily obtained from the above equation as a statistical mixture of the states  $D(v_e)S(\eta)|n\rangle$ , their weights depending on  $s$  and decreasing with  $n$ . Note that, because of the squeezing, states with  $n \neq 0$  are populated even at  $T=0$ , that is, in a purely quantum-noise regime.

### C. A qualitative discussion of the damping processes

The picture that emerges from the combination of both partial descriptions corresponds to a very simple quantum counterpart of classical bistability. The occurrence of two ‘‘attractors’’ has been imposed by construction: we have assumed the existence of two sets of differently displaced states as eigenstates of a system whose dissipative dynamics is modeled in the standard form of Eq. (8). Obviously, this approach, introduced merely as a tool formally convenient for tracing back some characteristics of dissipation to the Hamiltonian dynamics, is incomplete: since it does not give the transition between both representations, rooted in the strong nonlinearity of the problem, it cannot properly account for one of the main findings of Ref. [1], namely, the intrinsic monostable character of the quantum system, as opposed to the bistability of the classical analog. Now, let us show that, despite its evident limitations, the previous simplified treatment provides us with a framework for unraveling some features present in the complete system. Our qualitative understanding is summarized in the following points:

(i) First, we consider an initial state with a  $Q$  function located in the inner region of the phase space without overlapping the local-maximum area. As we have shown, in the displaced state basis, the deterministic system is approximately equivalent to an undriven anharmonic oscillator. Additionally, since, in this representation, the master equation retains the standard structure of Eq. (8), it follows that, in this region, the damping processes present no qualitative differences with the well-studied ones existent in the dissipative quartic oscillator [20–22]; in particular, the Gaussian  $Q$  function of an initial coherent state evolves into a ring of probability due to the nonlinearity and, eventually, into a Gaussian, which corresponds to the displaced vacuum if  $T=0$ .

(ii) For the system initially prepared in a coherent state centered on the local maximum, one of the cases treated in Ref. [1], a description in terms of displaced squeezed states can partially account for the different time scales detected in the numerical study [1]. There is a transient in which the evolution (damped oscillation) of the coherence between the two states that basically constitute the packet gives rise to partial revivals. More specifically, the system oscillates between the symmetric and the antisymmetric combinations, the period being  $t_{rev} \sim \pi/\sqrt{\delta\Omega_n}$ . The partial character of the revivals has a twofold origin: first, the nonlinear effects, which increase with  $n$ , lead to a fast dephasing of the part of the packet formed by the small contributions of other states; second, the damping of the coherence between the two main constituent states leads to a gradual variation in the shape of the packet. As the coherences decay to zero, the revivals eventually vanish. In a time scale  $\sim 1/\gamma_c$ , which corresponds to the characteristic time for the evolution of the populations in Eq. (11), an ‘‘asymptotic’’ state, given as a statistical mixture of the states  $D(v_e)S(\eta)|n\rangle$  with populations that depend on  $s$  and decrease with  $n$ , is formed. In this mixture, the squeezing in amplitude can be traced back to the squeezed character of each component. Moreover, since the eigenstates can be, in part, located on classically unstable areas [23], it is



understood how, for certain parameters, the distribution spills over the basin of the ground attractor. We emphasize that the transients, linked to the evolution of coherences and populations, disappear once the “steady” state around the maximum is reached, i.e., they die out on a time scale  $\sim 1/\gamma_c$ . The roots of metastability can also be conjectured: for a fixed Rabi frequency, the approximation found for the eigenstates becomes worse for increasing  $n$  and, at a certain point, the description of Eq. (11) fails, a slow loss of population taking place from the metastable state, which eventually may evolve in the way previously presented as characteristic of the inner region. An increase in the temperature gives rise to a transfer of population to higher levels, changing the weights in the mixture and accelerating the mechanism of loss (see Ref. [3] for a semiclassical derivation of the localization time).

(iii) Finally, in this framework, we can reasonably conjecture about the fast decay of an initial coherent state located beyond the metastability region [1]: in the outer regions of the phase space, displaced states  $D(v_g(n))|n\rangle$ ,  $v_g(n)$  varying smoothly with  $n$ , give a good description of the deterministic dynamics and, consequently, we can assume that, at least locally, a master equation with the standard form given by Eq. (9) applies. Hence, given the high values of the occupation numbers or equivalently of the energies, an initially very fast evolution of the coherences and a strong effect of the nonlinearity  $-1/2\delta(a^\dagger a)^2$  can be guessed. Obviously, given the approximate character of our study, we cannot clarify here important issues such as the precise definition of the quantum analogs of the classical basins of attraction; we can only stress the relevance to this point of the essential differences between the classical and the quantum formalisms. In this sense, it is worth recalling that, as opposed to the definition of a classical state as a point in the configuration space, which is unambiguously attached to one of the basins; in the quantum system, because of the finite extent of the wave functions, the  $Q$  function, even for an initially prepared eigenstate, can have parts in both classical basins.

We complete the analysis of dissipation by pointing out the applicability of our work to the exhaustive research carried out on the parallel system used to describe dispersive, optical bistability [9–12]; the methodology proposed in those studies, in particular, the characterization of the bistable and monostable regimes, is especially convenient for putting our approach on a more quantitative ground [11]; we have applied it and have checked how the range of parameters considered throughout our study corresponds, indeed, to an asymptotically monostable regime, the final state for  $T=0$  being a displaced vacuum, in agreement with our considerations.

#### IV. FIELD-CONTROLLED METASTABILITY

The knowledge of the specific dependence of the effects studied on the driving parameters allows a discussion of the possible use of the external field as a tool of control. In this sense, we summarize in the following some of the previously described properties, emphasizing how they are affected by

the frequency, phase, and intensity of the field.

(a) First, we remark that, for the appearance of metastability, the effective frequency  $\Delta$ , and the anharmonic potential must have different signs; additionally, as the magnitude of the displacement parameter  $v_e$  and, consequently, the mean occupation number of the metastable state are determined by  $\Delta$ ,  $\Omega_R$ , and  $\delta$ , proper values of  $\omega$  and  $\Omega_R$  must be chosen to guarantee the occurrence of “localization” in a particular range of energies. Furthermore, from the results obtained for the splitting of the eigenvalues, it follows that the time of revival of coherent states centered on the maximum can be altered by varying the values of  $\Omega_R$  and  $\Delta$ .

(b) The phase of the field,  $\varphi$ , fixes the phase of  $v_e$  and, in turn, the angular position of the localized distribution.

(c)  $\Omega_R$  affects also the validity of a linearization around the local maximum and the squeezing in the effective harmonic oscillator, higher Rabi frequencies improving the quality of the approximation; hence, the localization time and the spreading in phase can be controlled by adjusting the field intensity. Finally, it is also possible to change the displacement of the asymptotic state  $D(v_g)|0\rangle$ , basically, by varying the quotient between  $\Omega_R$  and  $\Delta$ .

#### V. CONCLUDING REMARKS

The study presented for the dissipative driven anharmonic oscillator gives an understanding of the mechanisms responsible for some aspects of the dynamics; furthermore, it provides some general clues to designing strategies of control. We have found that the unintuitive behavior emergent in the system is rooted in the effective enhancement of the nonlinear potential caused by the driving field: in the rotating-frame description, as the frequency is effectively reduced, the relative magnitude of the anharmonic term becomes significantly larger; additionally, since in this frame the master equation retains its standard structure, typical of linear and weakly nonlinear systems, the nontrivial features can be directly traced back to the high anharmonicity of the Hamiltonian system. Actually, this strong nonlinear character is reflected in the nonuniform properties of the eigenstate representation and in the complex topology of the corresponding phase space. Although approximate and only locally valid, our analysis provides enough information to clarify some points: near the “attractors” the mechanisms underlying the decay have been identified; an explanation for the appearance of partial revivals has been given; also, an almost exact characterization of the asymptotic state as a displaced state has been presented. The potential applicability of the study seems clear, given the predictive power of the analytical results obtained and the relevance of the model to real physical problems, particularly, to the cyclotron mode of an electron in a Penning trap.

#### ACKNOWLEDGMENT

S.B. wants to thank the Basque Government for financial support under Grant No. PI 1999-28.



- [1] D. Enzer and G. Gabrielse, Phys. Rev. Lett. **78**, 1211 (1997).
- [2] For a review, see L. S. Brown and G. Gabrielse, Rev. Mod. Phys. **58**, 233 (1986), and references therein.
- [3] B. Vestergaard and J. Javanainen, Phys. Rev. A **58**, 1537 (1998).
- [4] L. J. Lapidus, D. Enzer, and G. Gabrielse, Phys. Rev. Lett. **83**, 899 (1999).
- [5] S. Mancini and P. Tombesi, Phys. Rev. A **56**, R1679 (1997).
- [6] S. Mancini, A. M. Martins, and P. Tombesi, Phys. Rev. A **61**, 012 303 (1999).
- [7] S. Peil and G. Gabrielse, Phys. Rev. Lett. **83**, 1287 (1999).
- [8] M. Rigo, G. Alber, F. Mota-Furtado, and P. F. O'Mahony, Phys. Rev. A **58**, 478 (1998).
- [9] P. D. Drummond and D. F. Walls, J. Phys. A **13**, 725 (1980).
- [10] H. Risken, C. Savage, F. Haake, and D. Walls, Phys. Rev. A **35**, 1729 (1987).
- [11] H. Risken and K. Vogel, Phys. Rev. A **38**, 1349 (1988).
- [12] K. Vogel and H. Risken, Phys. Rev. A **38**, 2409 (1988).
- [13] F. A. M. de Oliveira, M. S. Kim, and P. L. Knight, Phys. Rev. A **41**, 2645 (1990).
- [14] J. Plata and J. M. Gomez Llorente, Phys. Rev. A **48**, 782 (1993); S. Brouard and J. Plata, *ibid.* **63**, 043 402 (2001).
- [15] H. P. Yuen, Phys. Rev. A **13**, 2226 (1976).
- [16] M. S. Kim, F. A. M. de Oliveira, and P. L. Knight, Phys. Rev. A **40**, 2494 (1989).
- [17] C. W. Gardiner, *Quantum Noise* (Springer-Verlag, Berlin, 1991).
- [18] C. Cohen-Tannoudji, J. Dupont-Roc, and G. Grynberg, *Atom-Photon Interactions: Basic Processes and Applications* (Wiley, New York, 1992).
- [19] F. Haake, H. Risken, C. Savage, and D. Walls, Phys. Rev. A **34**, 3969 (1986).
- [20] D. J. Daniel and G. J. Milburn, Phys. Rev. A **39**, 4628 (1989).
- [21] F. X. Kartner and A. Schenzle, Phys. Rev. A **48**, 1009 (1993).
- [22] S. Chatuverdi and V. Srinivasan, J. Mod. Opt. **38**, 777 (1991); Phys. Rev. A **43**, 4054 (1991).
- [23] J. Plata and J. M. Gomez Llorente, J. Phys. A **25**, L303 (1992).